European Review for Medical and Pharmacological Sciences 2012; 16: 1001-1012

The cell death pathway induced by metal halide complexes of pyridine and derivative ligands in hepatocellular carcinoma cells – necrosis or apoptosis?

G. KISMALI[1], F.M. EMEN[2], T. YESILKAYNAK[3], O. MERAL[1], D. DEMIRKIRAN[1], T. SEL[1], N. KULCU[3]

[1]Department of Biochemistry, Ankara University Faculty of Veterinary Medicine, Ankara-Turkey
[2]Department of Chemistry, Mehmet Akif Ersoy University Faculty of Arts and Science, Burdur-Turkey
[3]Department of Chemistry, Mersin University Faculty of Arts and Science, Mersin-Turkey

Abstract. – BACKGROUND, Drugs designed to restore programmed cell death might be effective against many cancer. It was aimed to study the possible apoptotic-necrotic effects of the pyridine-halide complexes such as dichlorodipyridinepalladium(II) ($PdCl_2L^1_2$), dichlorodipyridinenickel(II) ($NiCl_2L^1_2$), dichlorodipyridinecopper(II) ($CuCl_2L^1_2$), dibromodipyridinecopper(II) ($CuBr_2L^1_2$) and dichlorobis-(2,4-dimethylpyridine)copper(II) ($CuCl_2L^2_2$) in the hepatocarcinoma cells (Hep G2).

METHODS, All complexes were characterized by elemental analysis, 1H-NMR, FT-IR and Far-IR spectroscopy. Apoptotic effects were evaluated by cell viability assay, DNA laddering assay, LDH assay, DAPI nuclear staining and caspase 1-3-9 activity analysis.

RESULTS, According to cell proliferation/viability datas, $CuCl_2L^2_2$ was estimated the most toxic, $NiCl_2L^1_2$ the least toxic complex. Treatment of $CuCl_2L^2_2$ in IC_{50} doses resulted in a remarkable increase lactate dehydrogenase, it was followed by $CuBr_2L^1_2$ complex. Picnotic nuclei, anisonucleosis and nuclear condensations in 200 µM concentration of $CuCl_2L^2_2$ and $CuCl_2L^1_2$ treated cells were observed with DAPI staining also DNA brakes were also determined with electrophoresis. Caspase 1, 3 and 9 increased activation were not detected.

CONCLUSIONS, The present study results indicate that, $PdCl_2L^1_2$, $NiCl_2L^1_2$, $CuCl_2L^1_2$, $CuBr_2L^1_2$, $CuCl_2L^2_2$ complexes have antiproliferative action on hepatocellular carcinoma cells. However it would be wrong to interpret this effect as an apoptosis or necrosis exactly.

Key Words:
Metal halide complexes, Apoptosis, Hepatocellular carcinoma, Cell death, HepG2.

Introduction

Medicinal inorganic chemistry is a developing research area that began in 1962 with the synthesis of cis-diamminedichloroplatinum (II), later known as cisplatin. It is mainly used in the treatment of several types of cancer, including ovarian, head and neck, bladder, cervical and lymphoma. Several cisplatin analogs have been investigated as potential antitumor agents, but only two compounds (carboplatin and oxaliplatin) have entered clinical use worldwide[1-3]. Some palladium (II) complexes have been tested in animals bearing transplanted tumors. Although the activity of palladium complexes have generally been shown to be lower than that of platinum analogs with similar structures, many palladium (II) and palladium (I) neutral complexes were found to exhibit antitumor activity[4-6]. Transition metal-containing inorganic compounds are also considered to be potential carcinogens. Though nickel compounds are generally considered to be potentially carcinogenic, several nickel complexes have been tested for antitumor properties but were found to be inactive[7-9]. Inorganic copper complexes have been the subject of numerous antitumor studies, and many of these compounds have been found to be active as anticarcinogenic agents in animals. Such complexes include bisthiosemicarbazonates and monothiosemicarbazonates[10], oximes, imines and hydrazones[11-13], salicylates[14], aminocarboxylates[15] and other complexes with various N-donor ligands[16-17]. The biological activities of pyridine derivatives have been successfully studied for various biological actions. Metal halide complexes of pyridine derivatives such as 2-chloropyridine, 2-bromopyridine, 3-chloropyridine, 3-bromopyridine, 2-methoksipyridine[18], 2-(p-tolyl) pyridine[19], 2-methylpyridine, 3-methylpyridine, 3,4-dimethylpyridine[20], 4-benzoylpyridine, 3-hydroxypyridine, 4-ethylpyridine[21] have been extensive-

Corresponding Author: Gorkem Kismali, DM, Ph.D.; e-mail: gorkemkismali@yahoo.com

ly studied. However, the antitumor activities of these halide complexes have received less attention in the literature.

Hepatocellular carcinoma (HCC) is one of the most common malignancies worldwide, with an estimated more than half a million new cases per year[22]. HCC is an aggressive tumor that mostly occurs secondary to viral hepatitis infection, chronic liver disease and cirrhosis. With an estimated 711,000 new cases diagnosed annually, HCC is the fifth most common cancer worldwide and the third most common cause of cancer mortality[23]. A major obstacle to the treatment of HCC is the high rate of tumor recurrence after curative resection. Furthermore, effective palliative treatment is hindered by the fact that HCC is frequently resistant to conventional chemotherapy and radiotherapy[24].

Apoptosis, often used synonymously with the term ''programmed cell death,'' plays a crucial role in several physiological conditions and pathophysiological processes. It is a fundamental mechanism for the deletion of unwanted, senescent, or damaged cells[25-26].

Caspases, which play key roles in apoptosis, are synthesized as inactive zymogens and must be proteolytically cleaved at two aspartate residues to generate active, mature enzymes. The generation of active caspases forms a cascade in which "initiator" caspases interact with specific adapter molecules to facilitate their own autoprocessing. The active initiator caspases then in turn cleave and activate the downstream "executioner" caspases that cleave target substrates to orchestrate the proteolytic dismantling of the cell[27-29].

Based on their position in the apoptotic cascade, caspase-8, -9 and -10 are considered initiator caspases whereas caspase-3 and -7 are classified as executioner caspases. In contrast, caspases-1, -4 and -5 comprise the inflammatory caspases[30].

The development of tumors arise as a consequence of dysregulated proliferation and suppression of apoptosis. Many of the current chemotherapeutics designed to perturb proliferation do so in such a crude manner that the resulting damage to normal cells limits their clinical efficacy. However, targeting and overcoming abnormalities in tumor cells that suppress apoptosis could generate a potent proapoptotic stimulus by virtue of growth-deregulating mutations[29].

Apoptosis can be triggered by a variety of extrinsic and intrinsic signals such as cisplatin, doxorubicin, bleomycin, cytosine arabinoside, nitrogen, mustard, methotrexate, vincristine, gamma radiation, ultraviolet (UV) radiation, heat shock, viral infection, oxidants, free radicals, growth factor withdrawal, neurotransmitters and the Tumor Necrosis Factor (TNF) family of proteins[31].

This report describes the synthesis, cytotoxicity and apoptotic effects of dichlorodipyridinepalladium(II) ($PdCl_2L^1_2$), dichlorodipyridinenickel(II) ($NiCl_2L^1_2$), dichlorodipyridinecopper(II) ($CuCl_2L^1_2$), dibromodipyridinecopper(II) ($CuBr_2L^1_2$) and dichlorobis-(2,4-dimethylpyridine)copper(II) ($CuCl_2L^2_2$) complexes in the human hepatocellular carcinoma cell line HepG2.

Materials and Methods

Experimental

All chemicals were of analytical reagent grade. Metal halides ($PdCl_2$, $NiCl_2$, and $CuCl_2$), pyridine and 2,4-dimethylpyridine reagents were purchased from Merck. Solvents were purified according to standard procedures. Dichlorodipyridinepalladium (II) ($PdCl_2L^1_2$), dichlorodipyridinenickel(II) ($NiCl_2L^1_2$), dichlorodipyridinecopper(II) ($CuCl_2L^1_2$), dibromodipyridinecopper(II) ($CuBr_2L^1_2$) and dichlorobis-(2,4-dimethylpyridine)copper(II) ($CuCl_2L^2_2$) were synthesized as previously described[32-36]. The synthesis route of the metal (II) halide complexes with pyridine and 2,4-dimethyl pyridine is depicted in Figure 1.

Instrumentation

Infrared spectra were recorded in the range of 4000-400 cm^{-1} on a Mattson Satallite 5000 FT-IR spectrophotometer, equipped with Winfirst software (Mattson Instruments, Madison, WI, USA), using KBR pellets. Far infrared spectra were recorded in the range of 10-800 cm^{-1} on a Vertex 80V spectrophotometer (Bruker Optics, Ettlingen, Baden-Wurttemberg, Germany). All ^{1}H-NMR spectra were recorded on a Bruker Ultrashield Plus Biospin Avance III Mhz 400 NaNoBay FT-NMR spectrometer (Bruker Biospin, Ettlingen, Baden-Wurttemberg, Germany), using $CDCl_3$ as a solvent and tetramethylsilane (TMS) as an internal standard.

Synthesis of Complexes

Dichlorodipyridinepalladium(II) ($PdCl_2L^1_2$)

A solution of $PdCl_2$ (0.025 mol) in ethyl alcohol (40 mL) was added dropwise to a stirred and heated (70°C) solution of pyridine (0.05 mol) in ethyl alcohol (20 mL). The reaction mixture was

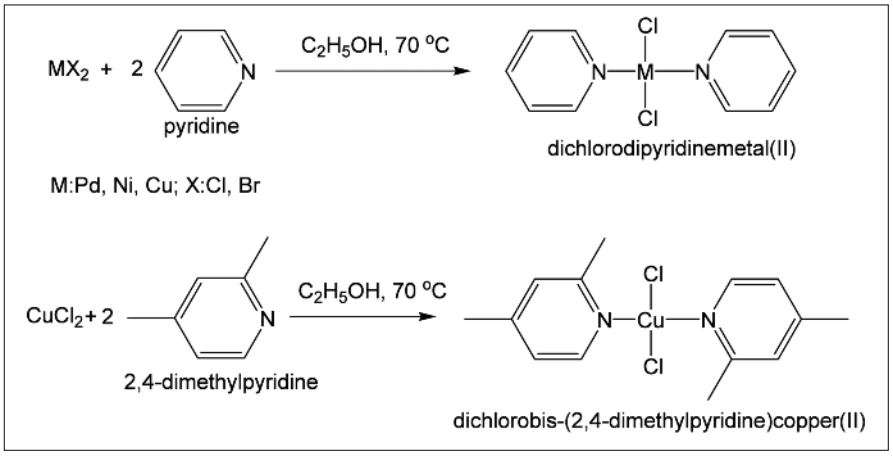

Figure 1. Scheme of the synthesis route of the metal(II) halide complexes of pyridine and 2,4-dimethylpyridine.

refluxed for 2 h at a 70°C and then cooled to allow for the precipitation of the complex compound. The complex that was obtained was filtered off, washed with ethyl alcohol and dried in a desiccator. Yield: 81%. Anal. Calc. for $PdC_{10}H_{10}N_2Cl_2$: C, 35.80; H, 3.00; N, 8.35. Found: C, 35.77; H, 3.10; N, 8.38.IR (KBr pellet, cm^{-1}): (C-C) 1607, (C-C) 1579. ^{1}H-NMR ($CDCl_3$): 8.76-8.78 (d, 4H, C-H), 7.71-7.73 (t, 2H, C-H), 7.26-7.30 (m, 4H, C-H).

Dichlorodipyridinenickel(II) ($NiCl_2L^1_2$)

A solution of $NiCl_2$ (0.025 mol) in ethyl alcohol (40 ml) was slowly added to a solution of pyridine (0.05 mol) in ethanol (20 ml). The reaction mixture was refluxed at 70°C for 2 h. The mixture was cooled until a precipitate was formed. The precipitate was filtered and then washed with ethyl alcohol and dried in a desiccator. Yield: 85%. Anal. Calc. for $NiC_{10}H_{10}N_2Cl_2$: C, 41.70; H, 3.50; N, 9.27. Found: C, 41.72; H, 3.49; N, 9.29. IR (KBr pellet, cm^{-1}): (C-C) 1606, (C-C) 1574. ^{1}H-NMR ($CDCl_3$): 8.73-8.8.77 (d, 4H, C-H), 7.70-7.73 (t, 2H, C-H), 7.25-7.33 (m, 4H, C-H).

Dichlorodipyridinecopper(II) ($CuCl_2L^1_2$)

A solution of $CuCl_2$ (0.025 mol) prepared in ethyl alcohol (40 ml) was added dropwise to a stirred solution of pyridine (0.05 mol) in ethanol (20 ml). The reaction mixture was refluxed for 2 h at 70°C and cooled for the precipitation of the complex compound. The obtained precipitation was filtered, washed with ethyl alcohol and dried in a desiccator. Yield: 81%. Anal. Calc. for $CuC_{10}H_{10}N_2Cl_2$: C, 41.05; H, 3.45; N, 9.57. Found: C, 41.04; H, 3.44; N, 9.57. IR (KBr pellet, cm^{-1}): (C-C) 1605, (C-C) 1574. Far-IR (cm^{-1}): (Cu-N) 266, (Cu-Cl) 289.

Dibromodipyridinecopper(II) ($CuBr_2L^1_2$)

This complex was prepared by a procedure similar to its chloro analogues. $CuBr_2$ (0.025 mol) was dissolved in ethyl alcohol (40 ml) and heated at 70°C with a magnetic stirrer and heater. Pyridine (0.05 mol) dissolved in ethanol (20 ml) was added to this solution dropwise, and then the mixture was refluxed at 70°C for 2 h. The reaction mixture was cooled for the precipitation of the complex compound. The obtained complex was filtered off, washed with ethyl alcohol and dried in a desiccator. Yield: 84%. Anal. Calc. for $CuC_{10}H_{10}N_2Br_2$: C, 31.72; H, 2.63; N, 7.36. Found: C, 31.48; H, 2.64; N, 7.34. IR (KBr pellet, cm^{-1}): (C-C) 1605, (C-C) 1574. Far-IR (cm^{-1}): (Cu-N) 254, (Cu-Cl) 266.

Dichlorobis-(2,4-dimethylpyridine)copper(II) ($CuCl_2L^2_2$)

A solution of $CuCl_2$ (0.025 mol) in ethanol (40 ml) was added dropwise to a stirred and heated (70°C) solution of 2,4-dimethylpyridine (0.05 mol) in ethanol (20 ml). The mixture was refluxed for 2 h at 70°C. The mixture was cooled to allow for the precipitation of the complex compound. The obtained complex was filtered off, washed with ethanol and dried in a desiccator. Yield: 80%. Anal. Calc. for $CuC_{14}H_{14}N_2Cl_2$: C, 48.21; H, 5.20; N, 8.03. Found: C, 48.21; H, 5.22; N, 8.06. IR (KBr pellet, cm^{-1}): (C-C) 1621, (C-C) 1560. Far-IR (cm^{-1}): (Cu-N) 250, (Cu-Cl) 312.

Cell Culture

The human hepatocellular carcinoma cell line HepG2 was purchased from ATCC (Wesel, Germany, Cat. HB-8065). HepG2 cells were maintained in Dulbecco's Modified Eagle (DME)

High Glucose media with 584 mg/L of L-Glutamine (Irvine Scientific,Santa Ana, CA, USA) containing 10% fetal bovine serum (Irvine Scientific,Santa Ana, CA, USA) and 50 µg/mL gentamycin sulfate solution (Irvine Scientific, Santa Ana, CA, USA). Cells were grown in 75 cm^2 vented cap flasks (BD Falcon, Rockville, MD, USA) in a humidified (5% CO_2) 37°C incubator. Medium was changed every two days. Cells were subcultured at a 1:4 ratio with trypsin-EDTA solution (Irvine Scientific, Santa Ana, CA, USA).

Cell Proliferation/Viability Assay

Cells were counted with a Neubauer hemocytometer. To study the viability and the injury of hepatomas, HepG2 cells were seeded in 96-well flat bottom cell culture plates (Greiner Bio One, Frickenhausen, Germany) at a density of 1×10^5 cells/well in 100 µL of culture medium. Cells were incubated in plates 24 h before the experiment to enable attachment. Dead or unattached cells were removed by washing out twice with phosphate buffered saline – PBS – (Irvine Scientific, Santa Ana, CA, USA) before all assays. A colorimetric assay was used for the quantification of cell proliferation and cell viability, based on the cleavage of the tetrazolium salt WST-1 to formazan by cellular mitochondrial dehydrogenases (The Quick Cell Proliferation Assay Kit, Biovision, San Francisco, CA, USA). The formazan dye produced by viable cells was quantified spectrophotometrically. Assays were performed according to the manufacturer's protocol. Briefly, cells were seeded in 96-well microtiter plates in a final volume 100 µL medium. Cells were incubated in normal cell culture conditions 24 h before each experiment. WST-1/Elecrocoupling solution (10 µL/well) was added to all control and experiment cell groups. After a 1 h incubation, absorbances were measured at 420-650 nm in a microtiter plate reader. The results were presented as the optical density. Each experiment was done in triplicate. Results were used to determination the IC_{50} values for each complex.

DAPI Nuclear Staining

For morphological observations, 1×10^6 cells/well in 1 mL of culture medium were seeded in 2-well chamber slides (Lab-Tek II Chamber Slide, Nunc, Rochester, NY, USA). The same subcultured cells were used in each experiment so that there was no effect of cell age on the experiment. The blue-fluorescent 4,6-diamidino-2-phenylindole (DAPI) nucleic acid stain preferentially stains dsDNA; it appears to associate with AT clusters in the minor groove. Binding of DAPI to dsDNA produces a ~20-fold fluorescence enhancement, apparently due to the displacement of water molecules from both DAPI and the minor groove. Changes in cell morphology and characteristics of apoptosis were examined by fluorescence microscopy of DAPI-stained cells (Leica DMI 4000, Wetzlar, Germany). The adherent monolayer cells were grown in two-well chamber slides. Cells were washed twice with PBS. DAPI stain (Gerbu, Wieblingen, Germany) was prepared at a 1:1000 dilution in Water for Injection (WFI) grade water and then added to the cells so that the cells were completely covered. Incubation was performed for 15 minutes at room temperature. At the end of the incubation period, the DAPI solution was aspirated and then the slides were washed once with PBS. The apoptotic nuclei (intensely stained, fragmented nuclei and condensed chromatin) were examined using a fluorescent microscope (Leica DMI 4000, Wetzlar, Germany) with 340-380 nm excitation.

DNA Fragmentation Assay

HepG2 cells were seeded in a 25 cm^2 culture flask. After the cell density reached 1×10^6 cells/mL, the cells were incubated with or without complexes (IC_{50}) for 24 h. After treatment, supernatants were collected to analyze the DNA damage in the deattached cells. The attached cells were trypsinized and collected by centrifugation (Sigma, 3-30K, Osterode am Harz, Germany). Pellets were washed with PBS, dissolved in lysis buffer (10 mM Tris-Cl, 1 mM EDTA, pH 7.4, 0.2% Triton X-100) and incubated at 37°C for 1 h in a heating block. At the end of the incubation period, cells were centrifuged at 20,000 × *g* for 10 min at 4°C. The cytoplasmic fraction (supernatant) was transfered to a clean tube. The pellet (nuclear DNA) left in the tube was dissolved in lysis solution and added to 0.1 mL of ice cold 5 M NaCl and 0.7 ml of ice cold isopropanol. Precipitation was allowed to occur for 1 hour in ethanol/dry ice. After precipitation, DNAs were recovered by centrifugation at 20,000 × *g*. Supernatants were discarded and the DNA samples were air dried. Samples were dissolved in buffer (10 mM Tris-Cl, 1 mM EDTA) and loading solution was added. All supernatants (top and bottom phases) were put in a heating block for 10 min at 65°C.

An agarose gel was prepared at a concentration of 1%. Ethidium bromide solution was added to samples and electrophoresis was then

conducted for 1 hour at 100 V in Tris-Acetic acid-EDTA (TAE) buffer. DNA bands were analyzed using UV light and a gel imaging system (Kodak Gel Logic 2200, Rochester, NY, USA).

Assessment of Cell Injury

Injury of HepG2 cells was quantified by measuring the release of lactate dehydrogenase (LDH) from lysed cells into the bathing medium. Cells (1×10^4 cells/well) were placed in 96-well plates and incubated with complexes for 24 h. Concentrations of supernatant LDH levels were determined using a commercially available colorimetric assay kit (TML Medical, Ankara, Turkey). A Clinical Chemistry Analyzer (ERBA XL 600, Meinheim, Germany) was used for the analysis. Total LDH release corresponding to complete HepG2 death was determined for each experiment. Each experiment was done in triplicate.

Caspase 1, Caspase 3 and Caspase 9 Assays

The caspase assays were based on the spectrophotometric detection of the chromophore p-nitroanilide (pNA) after cleavage from the labelled specific substrate YVDA-pNA, DEVD-pNA or LEHD-pNA. The pNA light emmision was quantified using a microtiter plate reader at 400-405 nm. Assays were performed according to the manufacturer's protocol (Caspase 1/ICE, Caspase 3/CPP32, Caspase 9 Colorimetric Assays, BioVision, San Francisco, CA, USA). Briefly, cells were seeded in 25 cm^2 flasks and labeled as control or treatment groups. Experimental cell groups were treated with complexes for 24 h with at the IC_{50} dose. Cells incubated without complexes were used as a control. Cells were collected by centrifugation and lysed with lysis buffer. Protein amounts were determined using the Bradford protein quantification method[37]. For each caspase assay, 100 µg of protein lysate was used. Reaction buffer and YVAD-pNA substrate were added and incubated 37°C for 1 h. Optical densities were read at 400 nm with a microtiter plate reader. All experiments were repeated three times. Caspase-1, -3 and -9 activities were determined by comparing the results of treated and control cells.

Results

Dichlorodipyridinepalladium(II) ($PdCl_2L^1_2$), dichlorodipyridinenickel(II) ($NiCl_2L^1_2$), dichlorodipyridinecopper(II) ($CuCl_2L^1_2$), dibromodipyridinecopper(II) ($CuBr_2L^1_2$) and dichlorobis-(2,4-dimethylpyridine)copper(II) ($CuCl_2L^2_2$) complexes were synthesized as previously described[32-36]. The reaction of the pyridine and 2,4-dimethylpyridine with metal halides (chloride and bromide) at 70°C with ethanol as the solvent yielded the complexes (Figure 1) The chemical structures of the complexes were verified by using elemental analysis, ^{1}H-NMR, FT-IR and Far-IR spectroscopy. ^{1}H-NMR spectra of copper complexes were not recorded because of their paramagnetic properties. Analytical and spectral data for the complexes are provided in the materials and methods section. The results are consistent with the proposed structures described in literature[32-36].

The effects of $PdCl_2L^1_2$, $NiCl_2L^1_2$, $CuCl_2L^1_2$, $CuBr_2L^1_2$ and $CuCl_2L^2_2$ complexes on the proliferation of HepG2 cells was investigated using the Quick Cell Proliferation Assay. The cell viability changes were found to depend on the concentrations and type of complexes. Results are shown in Figure 2. Complexes inhibited the proliferation of HepG2 human hepatocellular carcinoma cells in a concentration-dependent manner. Half-maximal inhibitory concentration (IC_{50}) values were determined for after a 24 h incubation. The following IC_{50} doses were determined: $NiCl_2L^1_2$ (175 µM), $CuCl_2L^1_2$ (88 µM), $CuBr_2L^1_2$ (125 µM) and $CuCl_2L^2_2$ (55 µM). All the complexes were dissolved in water for injection except for $PdCl_2L^1_2$. This complex was dissolved in dymethyl sulfoxide (DMSO), which has toxic effects on cells at high concentrations. The toxic dose of DMSO was determined to be 10% for HepG2 cells. $PdCl_2L^1_2$ was prepared at a maximum concentration of 200 µM; at higher doses, the compound was not soluble in DMSO. The toxic effect was therefore determined at 200 µM in HepG2 cells, but this effect does not depend solely on the palladium complex but also on the DMSO concentration. Thus the IC_{50} dose for dichlorodipyridinepalladium(II) could not be determined. Because the IC_{50} dose would be necessary for further apoptosis experiments, dichlorodipyridinepalladium(II) was, therefore, not examined in the following studies. According to cell proliferation/viability data, $CuCl_2L^2_2$ was determined to be the most toxic and $NiCl_2L^1_2$ was the least toxic complex.

Cell membrane damage was also monitored using the LDH leakage assay, because LDH is a stable cytosolic enzyme in normal cells and can leak into the extracellular fluid only after membrane damage. Exposure to complexes at IC_{50}

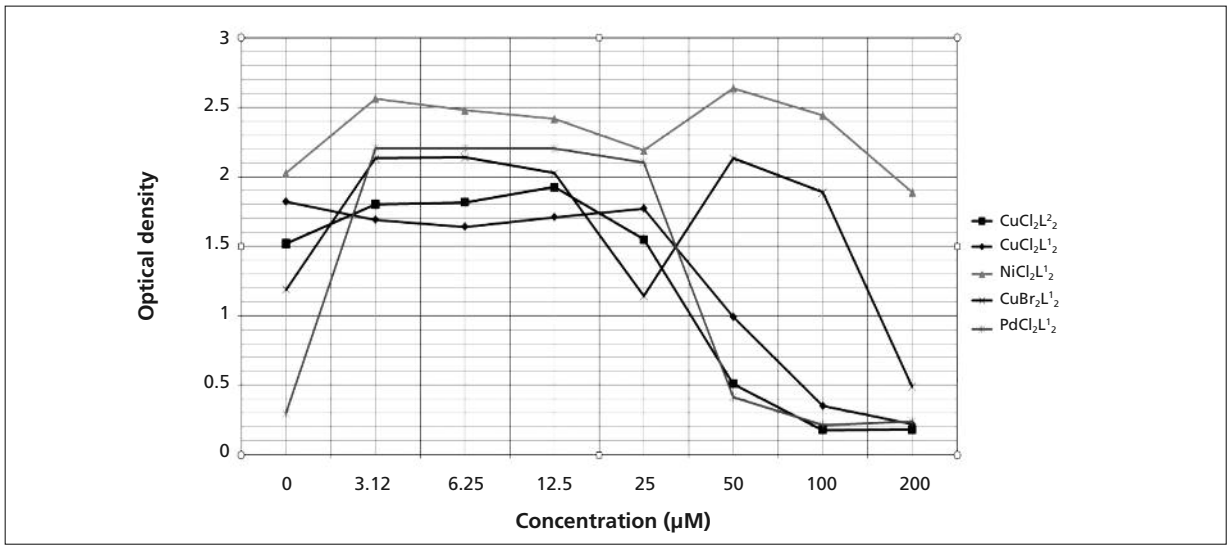

Figure 2. Dose dependent cell viability differentiation for dichlorodipyridinepalladium(II), Dichlorodipyridinenickel(II), Dichlorodipyridinecopper(II), Dibromodipyridinecopper(II), Dichlorobis-(2,4-dimethylpyridine) copper(II) in Hep G2 cell line for 24h incubation.

doses for 24 h resulted in LDH release from HepG2 cells to varying extents (Figure 3). Supernatant LDH levels (IU/mL) are provided in Table I. Treatment of dichlorobis-(2,4-dimethylpyridine)copper(II) at the IC_{50} dose resulted in a remarkable increase in LDH release; the amount of release was followed by the dibromodipyridinecopper(II) complex.

The nuclear morphology of the HepG2 cells was analysed using DAPI staining fluorescence microscopy. Chromatin cleavage was determined using conventional agarose gel electrophoresis (DNA laddering assay). DAPI is a *fluorescent stain* and is used extensively in *fluorescence microscopy*. When bound to double-stranded *DNA*, DAPI has its absorption maximum at 358 nm and its emission maximum at 461 nm.

We observed several picnotic nuclei, anisonucleosis and nuclear condensation in cells treated with 200 µM of dichlorobis-(2,4-dimethylpyridine) copper(II) and dichlorodipyridinecopper(II). This nuclear morphological change precedes chromatin condensation and can be dissociated from many early apoptotic events, such as DNA cleavage and cell shrinkage (Figures 4-8). These findings were dose-dependent, and DNA breaks were observed when a DNA laddering assay was used.

Endonuclease activation is a characteristic feature of apoptosis. This degrades genomic DNA at internucleosomal linker regions and produces 180 *base pair* DNA fragments. After *agarose gel electrophoresis*, this fragmentation gives a characteristic "laddered" appearance. In the present study, though the results do not show DNA laddering patterns as previously published, DNA drifts were observed on the agarose gels (Figures 9, 10).

Caspase-1 has been shown to induce cell *necrosis* or *pyroptosis* and may function in various developmental stages. Caspase-1 is *synthesize*d as a *zymogen* that is cleaved into 20 kDa (p20) and 10 kDa (p10) subunits that become part of the active enzyme. Caspase-1 activation was assayed and results were compared to untreated control cells. Changes were calculated as a percentage relative to the untreated control cells. Caspase-1 levels decreased 54, 37, 4 and 50% upon treatment with $CuBr_2L^1_2$, $CuCl_2L^1_2$, $NiCl_2L^1_2$ and $CuCl_2L^2_2$, respectively.

Caspase-9 is an initiator *caspase*. Once initiated, caspase-9 goes on to cleave *procaspase-3*. Caspase-9 activation was assayed spectrophotometrically and results were compared as a percentage to untreated control cells. Caspase-9 levels decreased 53, 35, 2 and 51% upon treatment with $CuBr_2L^1_2$, $CuCl_2L^1_2$, $NiCl_2L^1_2$ and $CuCl_2L^2_2$, respectively.

Caspase-3 is activated in apoptotic cells both by extrinsic (death ligand) and intrinsic (mitochondrial) pathways[38]. As an executioner caspase, the caspase-3 zymogen has virtually no activity until it is cleaved by an initiator caspase after apoptotic signaling events have occurred[39]. Caspase 3 activation was also assayed spectrophotometrically and results were compared to untreat-

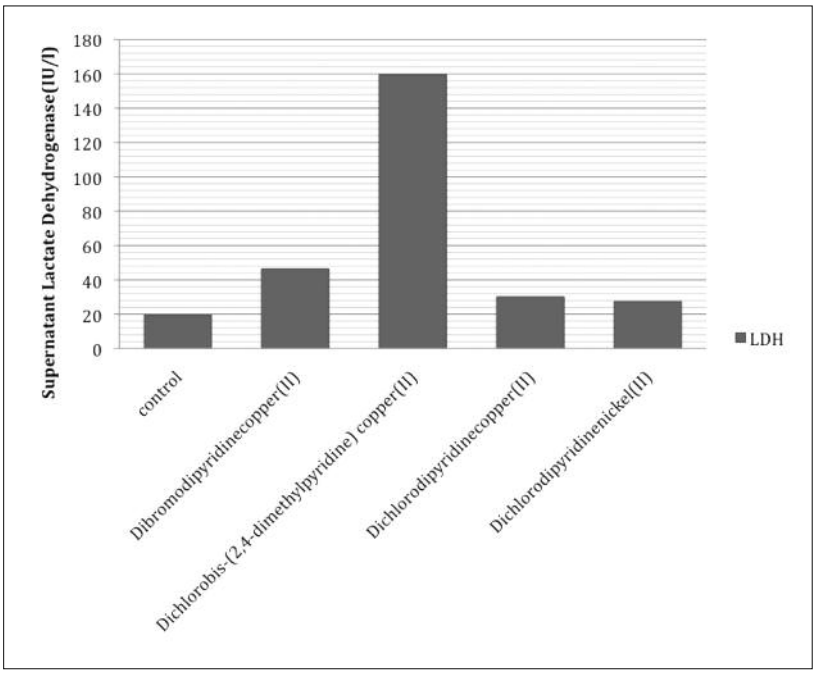

Figure 3. Cell culture supernatant lactate dehydrogenase (LDH) levels after 24h incubation period.

ed control cells. Caspase 1 levels decreased 75, 42, 8 and 54% upon treatment with $CuBr_2L^1_2$, $CuCl_2L^1_2$, $NiCl_2L^1_2$ and $CuCl_2L^2_2$, respectively.

Discussion

Drugs designed to restore programmed cell death may be effective against many cancers. Selective killing of tumor cells may be achievable with such drugs because unlike normal cells, cancer cells are under stress, destined to die, and highly dependent on aberrations of the apoptosis signalling pathways to stay alive.

Therapeutic strategies that induce the apoptotic process in various ways can be applied to cancer management. In the case of HCC, ursodeoxycholic acid (UDCA), used worldwide for the treatment of primary biliary cirrhosis and other chronic liver diseases, reduces hepatocarcinogenesis by inducing apoptosis of 'initiated hepatocytes' and by inhibiting proliferation[40].

The search for metal-based antitumor drugs resulted from the discovery by Rosenberg et al[41] in 1965 that cisplatin could effectively inhibit tumor growth. Cisplatin has subsequently become the most widely used anticancer drug in the world[42].

The compounds 2-acetylpyridine-N4-1-(4-fluorophenyl)piperazinylthiosemicarbazone, bis[2-acetylpyridine-N4-1-(4-fluorophenyl)piperazinylthiosemicarbazonato]zinc(II) and bis[l-acetato(2-acetylpyridine-N4-1-(4-fluorophenyl) piperazinylthiosemicarbazonato]zinc(II) were tested for their antiproliferative activity in vitro in the cells of four human cancer cell lines: HeLa (cervix adeno-

Table I. Cell culture supernatant lactate dehydrogenase (LDH) levels after 24 h incubation.

	Median	Min.	Max.
Control	15[a]	13	30
Dibromodipyridinecopper(II)	58[a]	13	68
Dichlorobis-(2,4-dimethylpyridine) copper(II)	142[b]	57	279
Dichlorodipyridinecopper(II)	19[a]	13	58
Dichlorodipyridinenickel(II)	35[a]	4	43

Data analysis was carried out using the SPSS 15 statistical package (SPSS, Chicago, IL, USA). The General Mann Whitney U test was applied to evaluate differences in the analyzed parameters. *Abbreviations*: [a]No significance; [b]Significantly different ($p < 0.05$).

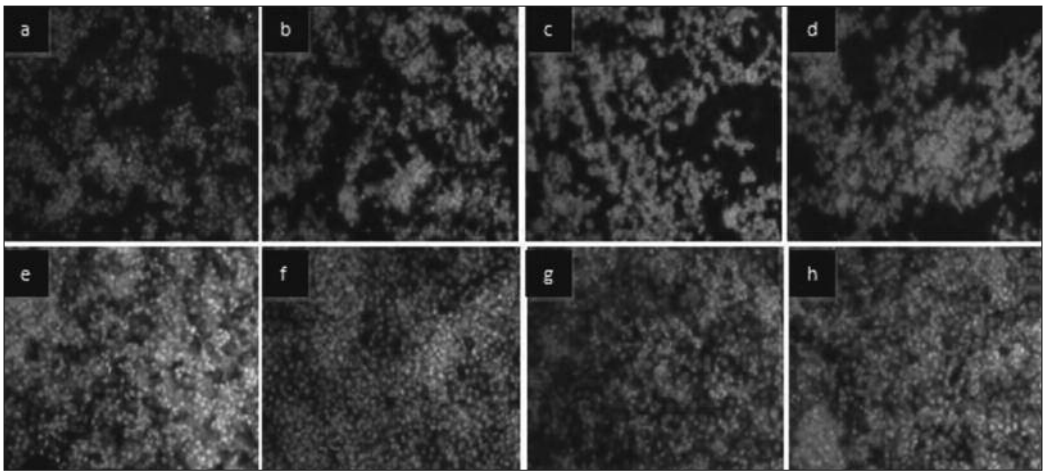

Figure 4. DAPI nuclear staining for dichlorodipy-ridinepalladium(II) doses. ***A,*** Control. ***B,*** 200 µM. ***C,*** 100 µM. ***D,*** 50 µM. ***E,*** 25 µM. ***F,*** 12.5 µM. ***G,*** 6.25 µM. ***H,*** 3.12 µM; 24h incubation.

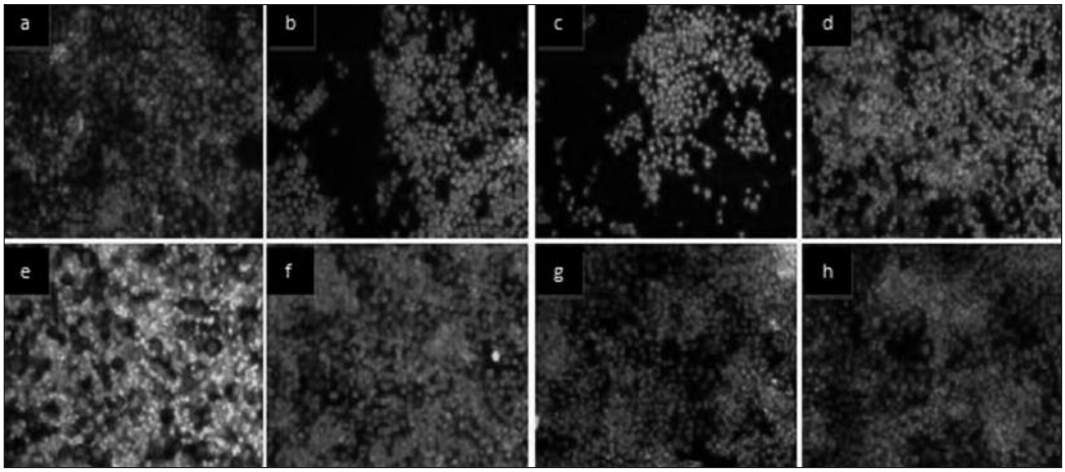

Figure 5. DAPI nuclear staining for dichlorobis-(2,4-dimethylpy-ridine) copper(II) doses. ***A,*** Control. ***B,*** 200 µM. ***C,*** 100 µM. ***D,*** 50 µM. ***E,*** 25 µM. ***F,*** 12.5 µM. ***G,*** 6.25 µM. ***H,*** 3.12 µM; 24h incubation.

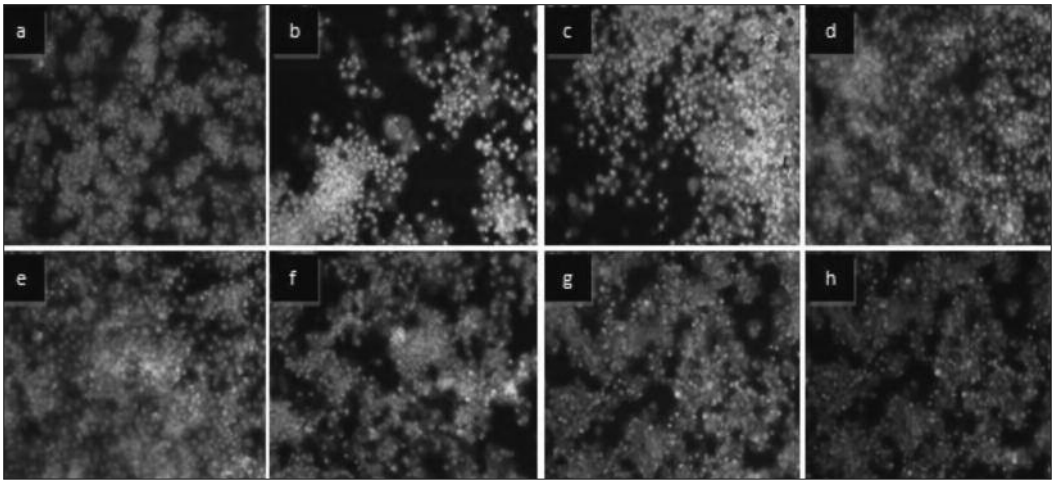

Figure 6. DAPI nuclear staining for dichlorodipy-ridinecopper(II) doses. ***A,*** Control. ***B,*** 200 µM. ***C,*** 100 µM. ***D,*** 50 µM. ***E,*** 25 µM. ***F,*** 12.5 µM. ***G,*** 6.25 µM. ***H,*** 3.12 µM; 24h incubation.

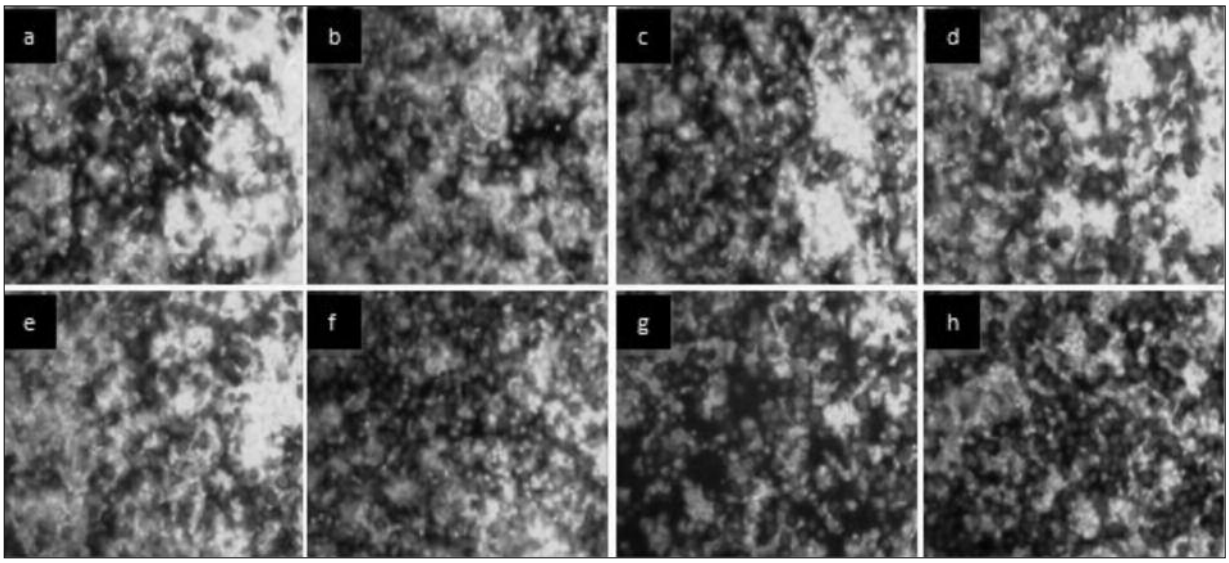

Figure 7. DAPI nuclear staining for dichlorodipyridinenickel(II) doses. ***A,*** Control. ***B,*** 200 μM. ***C,*** 100 μM. ***D,*** 50 μM. ***E,*** 25 μM. ***F,*** 12.5 μM. ***G,*** 6.25 μM. ***H,*** 3.12 μM; 24h incubation.

carcinoma cell line), K562 (chronic myelogenous leukaemia), MDA-MB-361 and MDA-MB-453 (breast cancer cell lines). Results showed that the ligand as well as the complexes demonstrated antiproliferative activities with IC_{50} values ranging from 26 to 90 nM. The compound 2-acetylpyridine-N4-1-(4-fluorophenyl)piperazinylthiosemicarbazone was shown to be 61 times more active than cisplatin in MDA-MB-361 and MDA-MB-453 cells and 303 times more active than cisplatin in HeLa and K562 cells[43].

The differences in the antiproliferative actions of $PdCl_2L^1{}_2$, $NiCl_2L^1{}_2$, $CuCl_2L^1{}_2$, $CuBr_2L^1{}_2$ and $CuCl_2L^2{}_2$ complexes indicate that the metal-halide complexes of pyridine or 2,4-dimethylpyridine have different antiproliferative activities

Treatment for 24 h with $NiCl_2L^1{}_2$, $CuCl_2L^1{}_2$, $CuBr_2L^1{}_2$ and $CuCl_2L^2{}_2$ complexes a IC_{50} doses effectively induce cell death. The form of cell death may be apoptotic cell suicide, with rounding and detachment of HepG2 cells. In addition

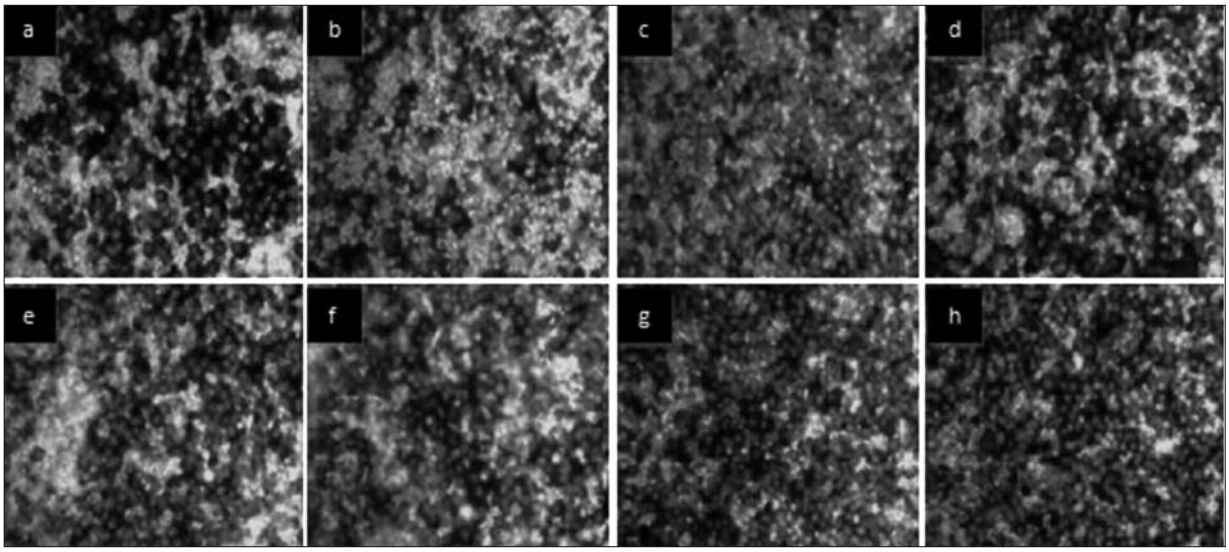

Figure 8. DAPI nuclear staining for dibromodipyridinecopper(II) doses. ***A,*** Control. ***B,*** 200 μM. ***C,*** 100 μM. ***D,*** 50 μM. ***E,*** 25 μM. ***F,*** 12.5 μM. ***G,*** 6.25 μM. ***H,*** 3.12 μM; 24h incubation.

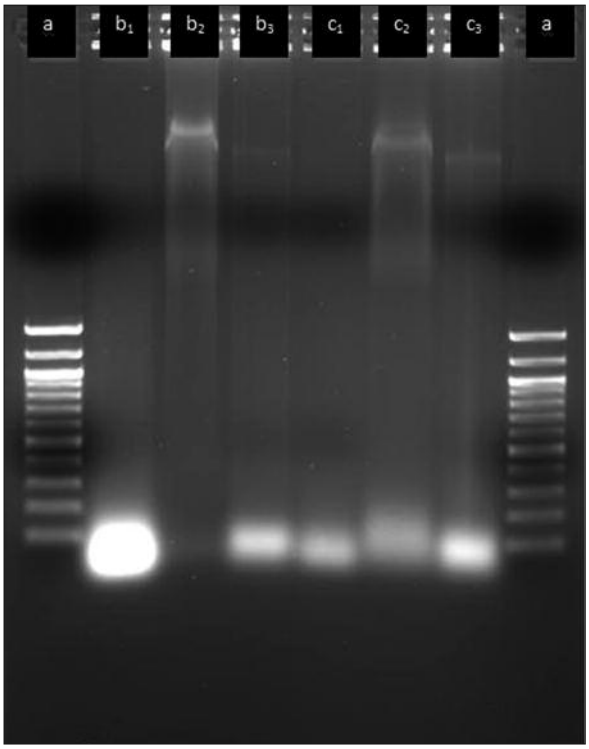

Figure 9. *a*, 100 bp DNA ladder. *b1*, $NiCl_2L^1_2$ top phase *b2*, $NiCl_2L^1_2$ supernatant phase. *b3*, $NiCl_2L^1_2$ bottom phase *c1*, $CuCl_2L^2_2$ top phase. *c2*, $CuCl_2L^2_2$ supernatant phase. *c3*, $CuCl_2L^2_2$ bottom phase.

to their growth inhibition activities, marked cytopathological effects, including spherical morphology and detachment of the cells, were observed in the Hep G2 cells treated with the metal halide complexes of pyridine or 2,4-dimethylpyridine. Stanojkovic et al[43] reported similar results for zinc(II) complexes of 2-acetyl pyridine 1-(4-fluorophenyl)-piperazinyl thiosemicarbazone and concluded that the cell death was due to apoptosis. However, apoptosis is a term that involves a series of biochemical events, such as caspase activation, that lead to specific changes in cell morphology. In the present study even though cell death was observed for all synthesized metal-halide complexes of pyridine or 2,4-dimethylpyridine with the MTT (4,5-*dimethylthiazol*-2-yl)-2,5-di*phenyl*-tetrazolium bromide) based cell viability assay, increased activation of caspases-1, -3 and -9 was not found. Thus it is difficult to conclude whether or not the cell death mechanism was apoptosis.

DNA fragmentation is one of the key features of apoptosis and also occurs in certain stages of necrosis. Apoptosis is characterized by the activation of endogenous *endonucleases* with subsequent cleavage of chromatin DNA into internucleosomal fragments of ~180 *bp*. This DNA fragmentation is analyzed by *agarose* gel *electrophoresis* to show a "ladder" pattern. *Necrosis*, on the other hand, is characterized by random DNA fragmentation which forms a "smear" on agarose gels. Pyridine-halide complexes, especially $CuCl_2L^1_2$ and $CuBr_2L^1_2$ caused DNA damage and a smear-ladder pattern. Histochemical studies such as the TUNEL assay may be necessary to make accurate conclusions.

Gokhale et al[44] tested the ligand and the copper complex for antitumor activity against the human breast cancer cell line MCF-7. Cells treated with N1-(2-benzyloxybenzylidene) pyridine-2-carboxamidrazone were shown to be growth arrested but viable, whereas those treated with cis-[dichloro-(N1-(2-benzyloxybenzylidene)pyridine-2-carboxamidrazone)copper(II) showed cell death at a comparatively low concentration, indicating a direct cytotoxic action. The IC_{50} value for the copper complex was 3 μM, which is four times less than that of the ligand. In our present study, the IC_{50} values that were determined were much higher than of Gokhale et al[44]. The sensitivity of cells to any of these stimuli can vary depending

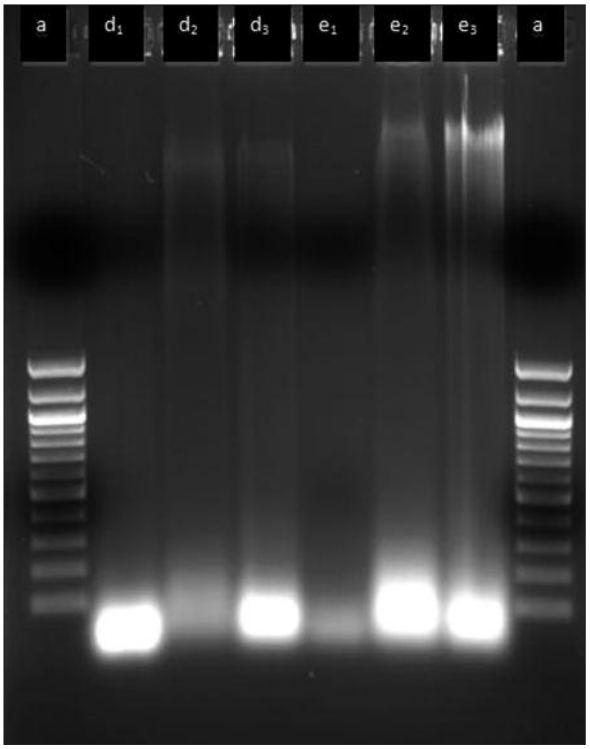

Figure 10. *a,* 100 bp DNA ladder. *d1*, $CuCl_2L^1_2$ top phase. *d2*, $CuCl_2L^1_2$ supernatant phase. *d3*, $CuCl_2L^1_2$ bottom phase *e1*, $CuBr_2L^1_2$ top phase. *e2*, $CuBr_2L^1_2$ supernatant phase. e3, $CuBr_2L^1_2$ bottom phase.

on a number of factors, such as the expression of pro- and anti-apoptotic proteins (e.g., the Bcl-2 proteins or the Inhibitor of Apoptosis Proteins), the severity of the stimulus and the stage of the cell cycle. Hepatocytes and hepatocellular carcinoma cells were more resistant than other cells against toxic agents.

Prachayasittikul et al[45] investigated the anticancer activities of the 1-adamantylthiopyridines in four cell lines: MOLT-3, HepG2, HuCCA-1 and A549. It was reported that 1-adamantylthionicotinic acid, its amide and nitrile derivatives were inactive in all the tested cell lines. On the other hand, 2-(1-adamantylthio)-5-hydroxypyridine and 3-(1-adamantylthio)-5-bromopyridine compounds have IC_{50} values of 35-41 μg/mL, respectively.

Targeting apoptosis is a promising strategy for cancer drug discovery. The present data will aid in future work. In investigating the agents that trigger apoptosis, the sensitivity of tumor cells will indicate the success of chemotherapies and the reduced costs of treatment.

References

1) Hambley TW. Metal-based therapeutics. Science 2007; 318: 1392-1393.
2) Storr T, Thompson KH, Orvig C. Design of targeting ligands in medicinal inorganic chemistry. Chem Soc Rev 2006; 35: 534-544.
3) Haiduc I, Silvestru C. Metal compounds in cancer chemotherapy. Coord Chem Rev 1990; 99: 253-296.
4) Cleare MJ, Hoeschele JD. Studies on the antitumor activity of group VIII transition metal complexes. Part I. Platinum(II) Complexes. Bioinorg Chem 1973; 2: 187.
5) Moawad MM, Anis SS, Eskander ML. Kinetics of interaction and complexation of the palladium(II) ion with new para-substituted-phenylazo-R-acid chromophores. Trans Met Chem 2001; 26: 50-56.
6) Gonzalez M, Terjero JM, Matilla A, Gutierrez JN, Fernandez MT, Lopez MC, Alonso C, Gonzalez S. Cis-Dichloro(α,ω-diamino carboxylate ethyl ester)palladium(II) as palladium(II) versus platinum model anticancer drugs: synthesis, solution equilibria of their aqua, hydroxo, and/or chloro species, and in Vitro/in Vivo DNA-binding properties. Inorg Chem 1997; 36: 1806-1812.
7) Rodriguez-Arguellez MC, Ferrari MB, Biscegli F, Pellizi C, Pelosi G, Pinell S, Sassi M. Synthesis, characterization and biological activity of Ni, Cu and Zn complexes of isatin hydrazones. J Inorg Biochem 2004; 98: 313-321.
8) Liang F, Zhou X, Li T, Li Z, Lin H, Gao D, Zheng C. Nickel(II) and cobalt(II) complexes of hydroxyl-substituted triazamacrocyclic ligand as potential antitumor agents. Bio Inorg Med Chem Lett 2004; 14: 1901-1904.
9) Afrasiabi Z, Sinn E, Lin W, Ma Y, Campana C, Padhye S. Nickel (II) complexes of naphthaquinone thiosemicarbazone and semicarbazone: Synthesis, structure, spectroscopy and biological activity. J Inorg Biochem 2005; 99: 1526-1531.
10) Zhang H, Wu JS, Peng F. Potent anticancer activity of pyrrolidine dithiocarbamate-copper complex against cisplatin-resistant neuroblastoma cells. Anticanc Drugs 2008; 19: 125-132.
11) Hall IH, Miller MC, Dothan XMA, Bouet FM. Cytotoxicity of copper complexes of 2-furaldehyde oxime derivatives in murine and human tissue cultured cell lines. Anticanc Res 1997; 17: 2411-2418.
12) Creaven BS, Czegledi E, Devereux M, Enyedy EA, Foltyn A, Karcz D, Kelett A, McClean S, Nagy NV, Noble A, Rockenbauer A, Planka TS, Walsh M. Biological activity and coordination modes of copper(II) complexes of Schiff base-derived coumarin ligands. Dalton Trans 2010; 39: 10854-10865.
13) Fan C, Su H, Zhao J, Zhang S, Miao J. A novel copper complex of salicylaldehyde pyrazole hydrazone induces apoptosis through up-regulating integrin β4 in H322 lung carcinoma cells. Eur J Med Chem 2010; 45: 1438-1446.
14) Palanisami N, Prabusankar G, Murugavel R. A novel dimeric copper salicylate with an undissociated COOH group: Synthesis and crystal structure of [Cu2(HSal)(Sal)(2,2'-bpy)2](ClO4). Inorg Chem Commun 2006; 9: 1002-1006.
15) Blower PJ, Lewis JS, Zweit J. Copper radionuclides and and radiopharmaceuticals in medicine. Nucl Med Biol 2006; 23: 957-980.
16) Huang R, Wallkvist A, Covel DG. Anticancer metal compounds in NCI's tumor-screening database: putative mode of action. Biochem Pharm 2005; 69: 1009-1039.
17) Devereux M, McCann M, O'Shea D, O'Connor M, Kiely E, McKee V, Naughton D, Fisher A, Kellett A, Walsh M, Egan D, Deegan C. Synthesis, superoxide dismutase mimetic and anticancer activities of metal complexes of 2,2-dimethylpentanedioic acid(2dmepdaH2) and 3,3 dimethylpentanedioic acid(3dmepdaH2): X-Ray crystal structures of [Cu(3dmepda)(bipy)]2·6H2O and [Cu(2dmepda)-(bipy)(EtOH)]2·4EtOH(bipy=2,2′Bipyridine). Bioinorg Chem Appl 2006; 1-11.
18) Mortimer CT, McNaughton JL. The thermal decomposition of transition metal containing heterocyclic ligands-substituted pyridine complexes of cobalt. Thermochim Acta 1974; 10: 125-128.
19) Allan JR, Carson BR. Thermal, spectral and magnetic studies of some first row transition metal complexes of 2-(p-tolyl)pyridine. Thermochim Acta 1990; 160: 329-335.

20) Farran R, House JE. Thermal decomposition of complexes of palladium(II) chloride with substituted pyridines. J Inorg Nucl Chem 1972; 34: 2219-2223.

21) Goher MAS. Thermal analysis of some cobalt(II) azido complexes of the type CoL4(N3)2 for L=pyridine derivative ligands. Thermochim Acta 1999; 336: 61-64.

22) Nagano H. Treatment of advanced hepatocellular carcinoma: Intraarterial infusion chemotherapy combined with interferon. Oncology 2010; 78: 142-147.

23) He AR, Soe K, Zouhairi KME. Current problems with systemic treatment of advanced Hepatocellular cancer. Curr Probl Canc 2010; 34: 131-149.

24) Kew M. Pathology/Diagnosis/Management. In: Sleisenger and Fordtran's Gastrointestinal and Liver Disease. Feldman M, Sleisenger M, Scharschmidt B, Klein S, Eds. WB Saunders, Philadelphia, 1998.

25) Kountouras J, Zavos C, Chatzopoulos D. Apoptosis in hepatocellular carcinoma. Hepatogastroenterology 2003; 50: 242-249.

26) Kountouras J, Zavos C, Chatzopoulos D. Apoptotic and anti-angiogenic strategies in live and gastrointestinal malignancies. J Surg Onc 2005; 90: 249-259.

27) Stennicke H, Salvesen G. Caspases–controlling intracellular signals by protease zymogen activation. Biophys Acta 2000; 1477: 299-306.

28) Nicholson D. Caspase structure, proteolytic substrates, and function during apoptotic cell death. Cell Death Differ 1999; 11: 1028-1042.

29) Kasibhatla S, Tseng B. Why target apoptosis in cancer treatment? Mol Cancer Therap. 2003; 2: 573-580.

30) Amer AO. Modulation of caspases and their non-apoptotic functions by Legionella pneumophila. Cell Microbiol 2010; 12: 140-147.

31) Thompson CB. Apoptosis in the pathogenesis and treatment of disease. Science 1995; 267: 1456-1462.

32) Szecsenyi KM, Wadsten T, Carson B, Bencze E, Kenessey G, Liptay G. Pyridine type complexes of transition metal halides, XIII. Solid-state studies of copper(II)-chloride and bromide complexes with methylpyridines. Part II: complexes with 2- and 4-methylpyridine and 2,4,6-collidine. Thermochim Acta 1999; 340-341: 255-261.

33) Allan JR, Brown DH, Nutall RH, Sharp DWA. The far infra-red spectra of some transition metal halide complexes with substituted pyridines. J Inorg Nucl Chem 1965; 27: 1305-1309.

34) Allan JR, Brown DH, Nutall RH, Sharp DWA. The preparation and thermal decomposition of some pyridine and substituted-pyridine complexes of nickel(II) halides. J Inorg Nucl Chem 1965; 27: 1529-1536.

35) Szecsenyi KM, Wadsten T, Carson B, Bencze E, Kenessey G, Gaal FF, Liptay G. Pyridine type complexes of transition metal halides, XII. Solid state studies of copper(II)-chloride and bromide complexes with methylpyridines. Part I: Complexes with 3-methylpyridine. Thermochim Acta 1998; 316: 75-78.

36) Liao CY, Lee HM. Trans-Dichlorodipyridinepalladium(II). Acta Cryst 2006; 62: 680-681.

37) Stoscheck C. Quantification of protein. Methods Enzymol 1990; 182: 50-68.

38) Salvesen GS. Caspases: opening the boxes and interpreting the arrows. Cell Death Differ 2002; 9: 3-5.

39) Walters J, Pop C, Scott FL, Drag M, Swartz P, Mattos C, Salvesen GS, Clark AC. A constitutively active and uninhibitable caspase-3 zymogen efficiently induces apoptosis. Biochem J 2009; 424: 335-345.

40) Oyama K, Shiota G, Ito H, Murawaki Y, Kawasaki H. Reduction of hepatocarcinogenesis by ursodeoxycholic acid in rats. Carcinogenesis 2002; 23: 885-892.

41) Rosenberg B, Loretta VC, Thomas K. Inhibition of cell division in Escherichia coli by electrolysis products from a platinum electrode. Nature 1965; 205: 698-699.

42) Auzias M, Therrien B, Suss-Fink G, Sÿtepnicka P, Ang WH, Dyson PJ. Ferrocenoyl pyridine arene ruthenium complexes with anticancer properties: Synthesis, structure, electrochemistry and cytotoxicity. Inorg Chem 2008; 47: 578-583.

43) Stanojkovic TP, Kovala-Demertzi D, Primikyri A, Garcia-Santos I, Castineiras A, Juranic Z, Demertzis MA. Zinc(II) complexes of 2-acetyl pyridine 1-(4-fluorophenyl)-piperazinyl thiosemicarbazone: Synthesis, spectroscopic study and crystal structures - Potential anticancer drugs. J Inorg Biochem 2010; 104: 467-476.

44) Gokhale N, Padhye S, Rathbone D, Billington D, Lowe P, Schwalbe C, Newton C. The crystal structure of first copper(II) complex of a pyridine-2-carboxamidrazone-a potential antitumor agent. Inorg Chem Commun 2001; 4: 26-29.

45) Prachayasittikul S, Treeratanapiboon L, Ruchirawat S, Prachayasittikul V. Novel activities of 1amantylthiopyridine as antibacterials, antimalarials and anticancers. EXCLI J 2009; 8: 121-129.